EFFECTS OF DISPERSION PROPERTIES ON TRANSMISSON LOSS OF THICK PANELS

Katsuya Matsuzaki

Shikayama, Midori-Ku, Nagoya, Japan, mats@s2.dion.ne.jp

ABSTRACT

For thick panels under certain conditions, continually low values of transmission loss can be shown in the high frequency range. This effect has been thought to be due to the shear type wave coincidence effect. In this work, the dispersion properties of thick panels are precisely investigated to get a right explanation for this phenomenon and to determine conditions in which this phenomenon occurs. It is also shown that lowering the stiffness of the panels is not always an effective approach to improving the transmission loss for thick panels though the approach is well-known to be effective for thin panels and has been also proposed for thick panels.

I. INTRODUCTION

The sound transmission of various kinds of panels has been extensively studied. In previous studies, the wave speed in a panel is often treated as one of the key factors to determine the transmission behaviour of panels. The bending wave of a panel is well known as a cause of the coincidence phenomenon. In addition, for certain types of panels, such as sandwich panels, the shear wave of a panel plays an important role in determining the transmission behaviour. A simple impedance model for sandwich panels was prepared by Kurtze & Watters[1], and this model suggests that if the shear wave speed in a panel coincides with the speed of sound in air, it causes a drastic decrease in the transmission loss (TL). Many researchers have treated this type of coincidence [2-6]. A similar type of phenomenon exists in thick single layer panels. Sharp presented a simple impedance model for thick panels to explain this phenomenon[7]. In this model, shear wave impedance has been treated as a key factor for explaining for the transmission characteristics of thick panels, but this model cannot provide a proper explanation for characteristics peculiar to the high frequency range transmission loss of thick panels and this model does not provide proper measures for improving the noise reduction capability of panels. In this work, the aim is to understand properly the transmission characteristics of thick panels and to provide the a proper noise control measure for them. For an infinite elastic panel, the analytical solution for TL exist [8-10]. Based on this solution, the dispersion properties of thick panels are precisely investigated, and the exact conditions under which the high frequency range TL decreases most drastically are shown. And It is also shown that lowering the stiffness of the panels is not an effective approach to improving the transmission loss for thick panels though the approach is well-known to be effective for thin panels and it has been also proposed for thick panels.

II. SHARP'S IMPEDANCE MODEL FOR THICK PANELS

Sharp provided the following impedance model for thick panels [7].

$$Z \approx \mathrm{j}\omega\rho_m h + \frac{Z_B Z_S}{Z_B + Z_S} \tag{1}$$

Z_B and Z_S are respectively called the bending wave impedance and the shear wave impedance and are described as follows.

$$Z_B = -\mathrm{j}\frac{\left\{\dfrac{Eh^3}{12(1-\nu^2)}\right\}\omega^3 \sin\theta^4}{{c_0}^4}$$

$$Z_S = -\mathrm{j}\frac{Gh\sin\theta^2}{{c_0}^2} \tag{2}$$

where E is the Young's modulus, ν is the Poisson ratio , ω is the angular frequency, θ is the sound incident angle, c_0 is the speed of sound in air, G is the second Lame coefficient, namely, the shear modulus, and h is the panel thickness.

The forcing in-plane wave speed c is given by $c=c_0/\sin\theta$

Using this relation and letting the impedance Z, shown as equation (1), be 0, the dispersion curve, which shows the dependence of the generated wave speed in a panel on the frequency of an input force, can be obtained. Sharp discussed the TL characteristics of three hypothetical panels with different properties [7]. Thus, the TL characteristics of panels A, B and C, shown in Table 1, will be discussed. Panels A, B and C have the shear wave speed

$\sqrt{G/\rho}$ respectively higher than, the same as and lower than the forcing in-plane wave speed caused by sound incidence at the angle of 78°. An angle of 78° is the upper limit angle for estimating the field incident TL, and the angle that characterises the field incidence TL has physical meaning in a sense [11,12] and was therefore selected for the incident angle in this investigation.

The dispersion curves obtained for these panels are shown in Figure 1. In the high frequency range, the shear wave is dominant, and the wave propagating speed in the panel is constant. If the wave propagating speed coincides with the forcing wave speed by the sound incidence, as in the case of panel B, it is expected that TL reduction in the high frequency range occurs broadly, as suggested by Sharp.

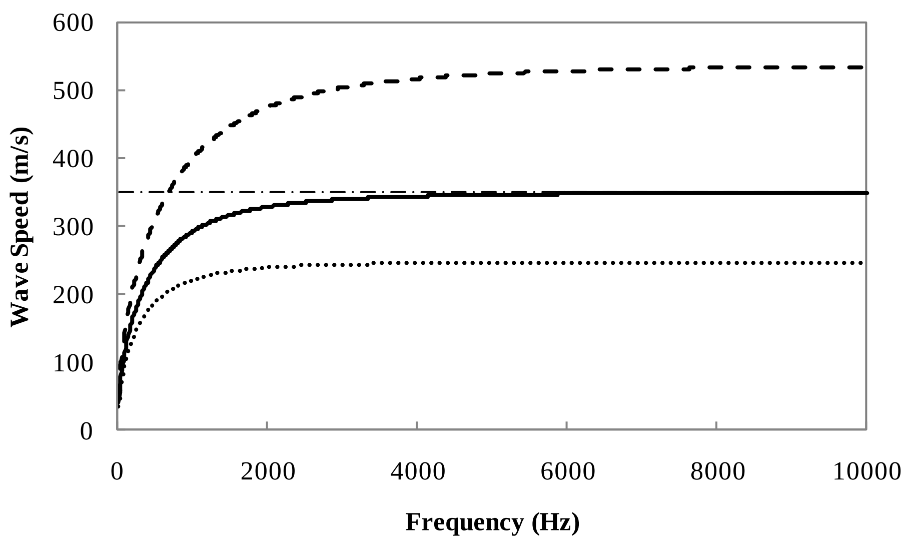

FIG.1. Dispersion curves of panels estimated based on Sharp's impedance model.

------, Panel A ; ——, Panel B ; ··········,Panel C ; -·-·-·,forced wave speed by 78°incidence sound.

The TL characteristics can be directly evaluated from the panel impedance based on the method [13] described in Appendix A. The TL curves thus obtained for A, B and C are shown in Figure 2. In this estimation, the value 1.21 kg/m^3 is used for the air density ρ_0. The loss factor η is assumed to be 0.02 using complex elasticity $E(1+j\eta)$, $G(1+j\eta)$ in equation (2). These results are similar to the schematic graph prepared by Sharp [7]. For panel B, in which the wave propagating speed coincides with the forcing wave speed due to the sound incidence, TL reduction in the high frequency range is observed. On the other hand, for panel C, in which the shear stiffness is sufficiently low, there is no dip in the TL curve.

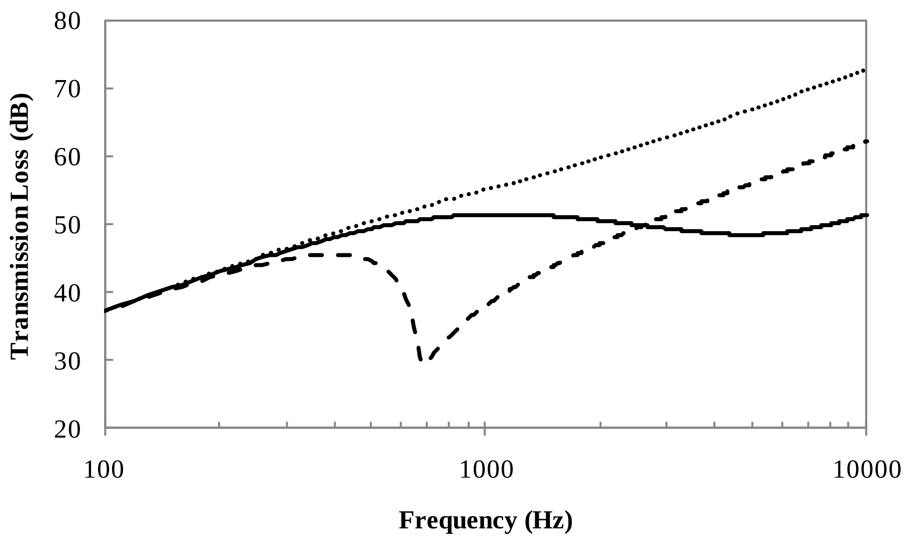

FIG.2. TL properties estimated based on Sharp’s impedance model.

------, Panel A ; ——, Panel B ; ··············, Panel C.

III. EVALUATION OF SHARP'S MODEL BASED ON ANALYTICAL SOLUTIONS

For an infinite elastic panel, an analytical solution for the TL exists. The details of the analytical model are shown in Appendix B. This model is equivalent to the existing approaches [8-10]. Thus, Sharp's impedance model can be evaluated by comparison with this analytical model. Firstly, the dispersion characteristics will be investigated. The dispersion curve can be obtained for a panel by letting Z , the (1,2) component of the (B-6) matrix in Appendix B, be 0. The dispersion curve obtained for panel B with such a procedure is shown in Figure 3. Precisely, the graph shows the counter of $1/|Z|$. The branches in the dispersion curve can be observed in it. The overall aspects of the branches are similar to the results obtained previously for a thick panel [14]. In the high frequency range, part of the constant wave speed is observed in this curve. In the figure, the dispersion curve based on Sharp's impedance model is overwritten. The velocity of the flat part in this dispersion curve is slightly lower than that obtained from Sharp's impedance. In the high velocity range, there are many branches that cannot be observed in the dispersion curve given by Sharp's impedance. These features are common for dispersion curves of single-layer thick panels that have the flat part of the dispersion curves in the audible frequency range.

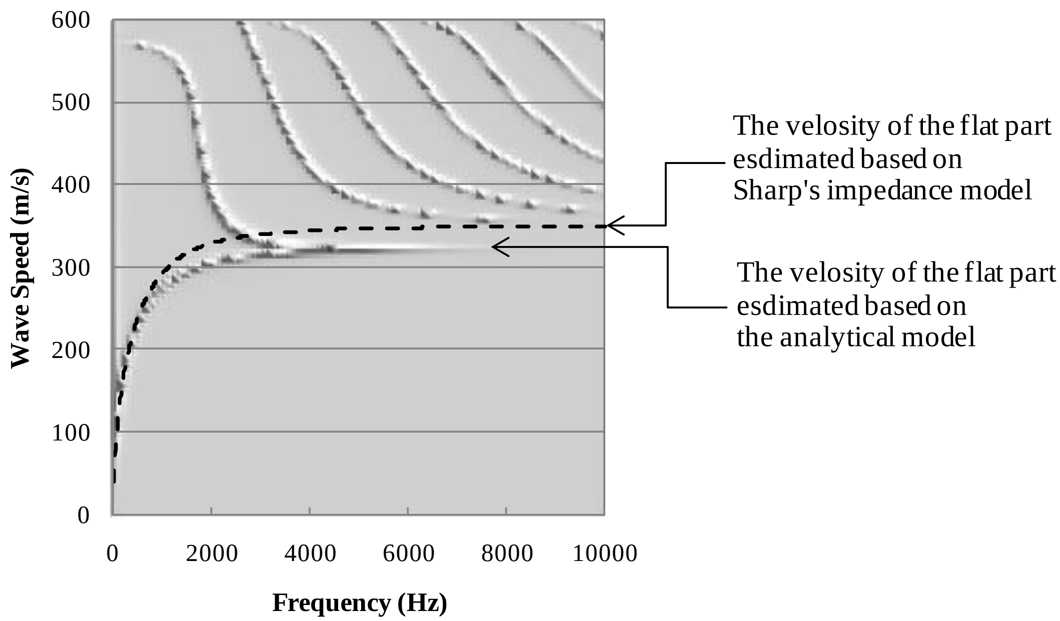

FIG.3. Dispersion curve of panel B estimated based on the analytical solution shown as the inverse of the impedance and the estimation based on Sharp's impedance model.------.

A. DISPERSION CURVE CHARACTERISTICS

The velocity of flat portion in the dispersion curve coincides with the Rayleigh velocity[14]. This is also shown as follows.

In Appendix B, the detailed expression of the (1,2) component of the (B-6) matrix is shown. The following K_0 part determines the sign of this component. The sign of the other parts are constant in the condition in this investigation.

$$K_0 = K_1\left\{4\alpha\beta\xi^2 + \left(\xi^2 - \beta^2\right)^2\right\} + \left(K_2 - K_1\right)\left\{8\alpha\beta\xi^2\left(\xi^2 - \beta^2\right)^2\right\} \tag{3}$$

where K_1 and K_2 are as follows.

$$K_1 = \sin(\alpha h)\sin(\beta h)$$

$$K_2 = 1 - \cos(\alpha h)\cos(\beta h)$$

K_0 mainly consists of the real part with a negative sign. In the velocity range in which the flat part in the dispersion curve exists, the sign of K_0 changes to be positive only in a very local velocity range. The first term in K_0 usually has a minus sign, and it becomes 0 only at the Rayleigh velocity [14]. The second term is always a very small, positive value. Thus, at the two points of velocity near the Rayleigh velocity, the sign of K_0 changes, and the (1,2) component becomes 0. In Fig. 3 the two separated branches are not observed clearly. However, it can been seen that the zone in which the impedance is zero exists near the Rayleigh velocity. When the Poisson's ratio is 0.25, the analytic solution of the Rayleigh velocity exists. The velocity of the flat part in the dispersion curve, which implies the zero impedance region, coincides with the Rayleigh velocity $\sqrt{2-2/\sqrt{3}}\sqrt{G/\rho}$ obtained analytically. When the velocity of the flat part in the dispersion curve coincides with the forcing velocity due to the incident sound, the TL reduction in the high frequency range occurs. Thus, the velocity of the flat part is the important factor that determines the TL characteristics. In this investigation, the velocity is shown to be near the Rayleigh velocity $\sqrt{2-2/\sqrt{3}}\sqrt{G/\rho}$ rather than near the shear wave speed $\sqrt{G/\rho}$ Sharp suggested. In general, the Rayleigh velocity is a little less than the speed of the shear wave, and it is well-known to be approximated as $(0.87+1.12\nu)/(1+\nu)\sqrt{G/\rho}$. For example, in the case that the Poisson's ratio is 0.2, the Rayleigh velocity is about 10% less than the shear wave speed. Estimating this velocity base on Sharp's model results in an erroneous estimation. When the G/ρ value with which this type of coincidence occurs is estimated, the estimated value based on Sharp's model can be about 20% lower than true value that is based on the analytical solution.

B. PLANE WAVE TRANSMISSION

To show the relation between the dispersion curve in Fig. 3 and the TL characteristics, the transmission of plane waves at a single incident angle is estimated. The angle of the incident wave is arbitrary, but 78° is the angle that characterises the field incidence TL in the next section, so it was selected for the incident angle in this investigation.

Five hypothetical types of panels whose properties are shown in Table 1 were selected for evaluating TL characteristics. The dispersion curves for these panels based on the analytical model are shown in Figure 4. The forcing wave velocity caused by incident sound at the angle of 78° is over-written. The five types of panels have different types of relationships between the forcing wave velocity and the flat part of the velocity in the dispersion curve. The TL of each panel was calculated for 78° incident sound with a 0 loss factor condition and 0.02 loss factor condition. These results are shown in Figure 5. In each case, a matrix that characterises wave transmission was given by equation (B-6) in Appendix B. Then, TL is calculated with equation (A-3) in Appendix A. It is clearer in the 0 loss factor condition that Type B', which has a Rayleigh wave speed coincident with the forcing wave speed, has a wider frequency range of the dip than type B, which has a shear wave speed that is the same as the forcing wave speed. Nearly the same tendency is confirmed in the case with the 0.02 loss factor. In contrast with Sharp's results, shown in Figure 2, many dips in TL are observed for panel C, which is in the condition where the velocity of the flat part of the dispersion curve is sufficiently lower than the forcing wave speed because of the many branches in the higher velocity range over the flat part in the dispersion curve.

TABLE I. Panel Properties

Type	G(N/m^2)	Wave Speed Condition
A	3.491e8	$\sqrt{\frac{G}{\rho}} > c_0 / \sin(78°)$
B’	1.746e8	$\sqrt{(2-\frac{2}{\sqrt{3}})\frac{G}{\rho}} = c_0 / \sin(78°)$
B”	1.602e8	$\frac{1+\sqrt{(2-\frac{2}{\sqrt{3}})}}{2}\sqrt{\frac{G}{\rho}} = c_0 / \sin(78°)$
B	1.476e8	$\sqrt{\frac{G}{\rho}} = c_0 / \sin(78°)$
C	7.378e7	$\sqrt{\frac{G}{\rho}} < c_0 / \sin(78°)$

Note: ρ=1200kg/m^2 , h=0.15m , ν=0.25 , c_0=343m/s

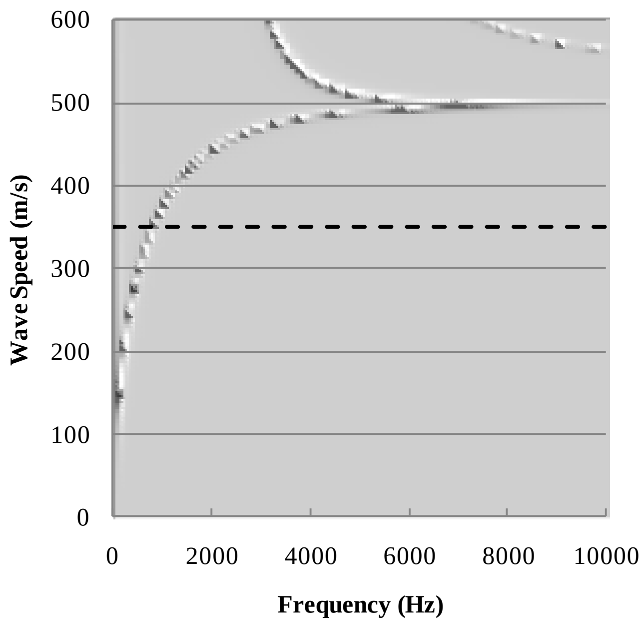

(a) Estimation for panel A

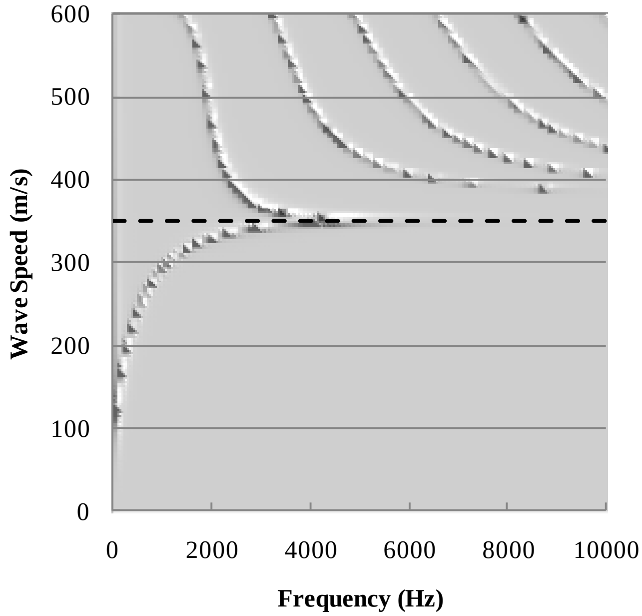

(b) Estimation for panel B'

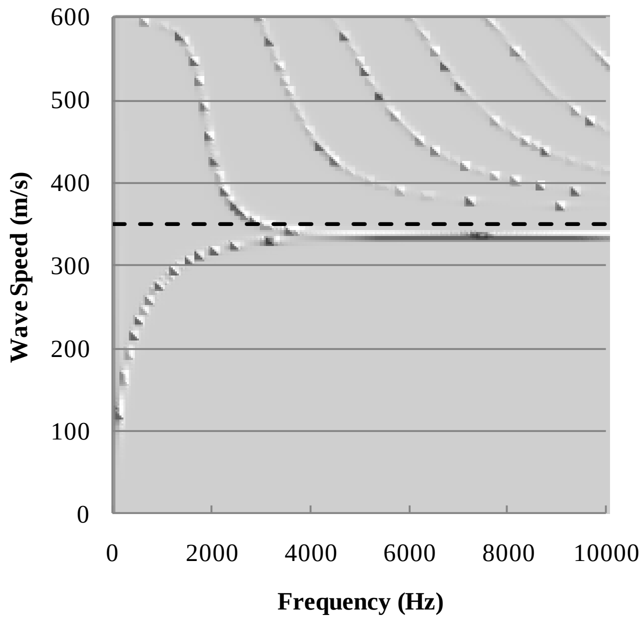

(c) Estimation for panel B"

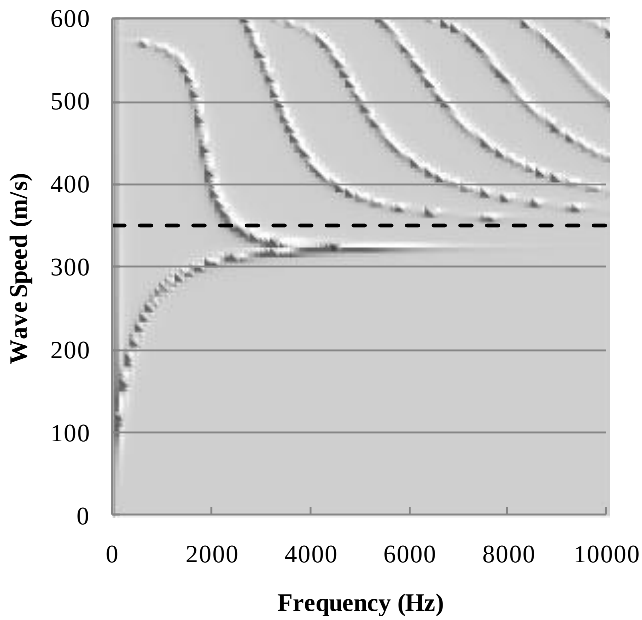

(d) Estimation for panel B

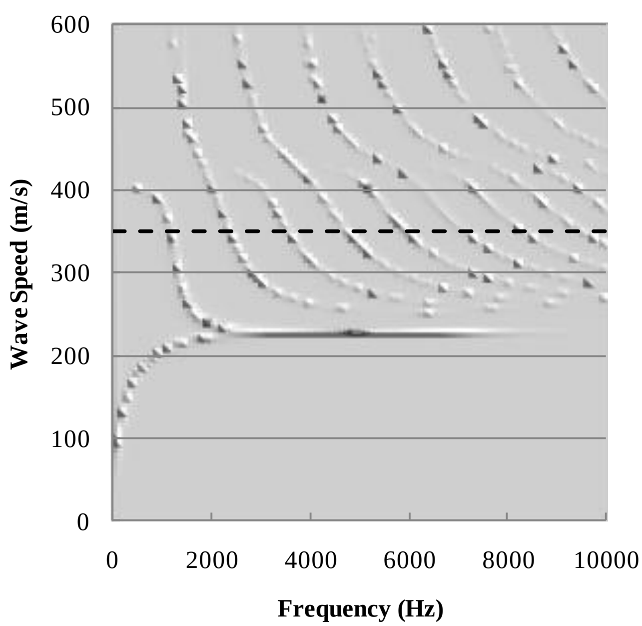

(e) Estimation for panel C

FIG.4. Dispersion curves of panels estimated based on the analytical solution shown as the inverse of the impedance and forced wave speed with 78°incidence sound.------.

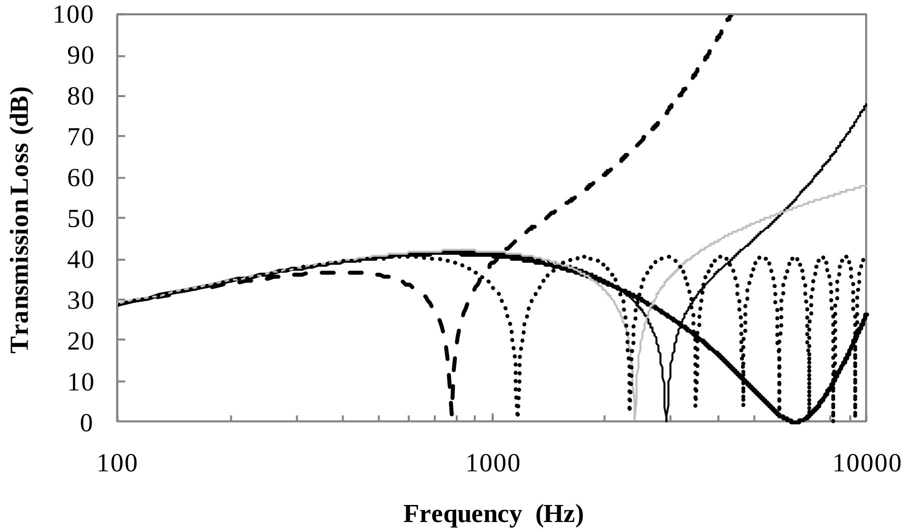

FIG.5. TL properties estimated based on the analytical solution for 78°sound incidence with the panel loss factor η=0.

------, Panel A ; ——, Panel B' ; ——, Panel B" ; ——, Panel B ; ··········, Panel C.

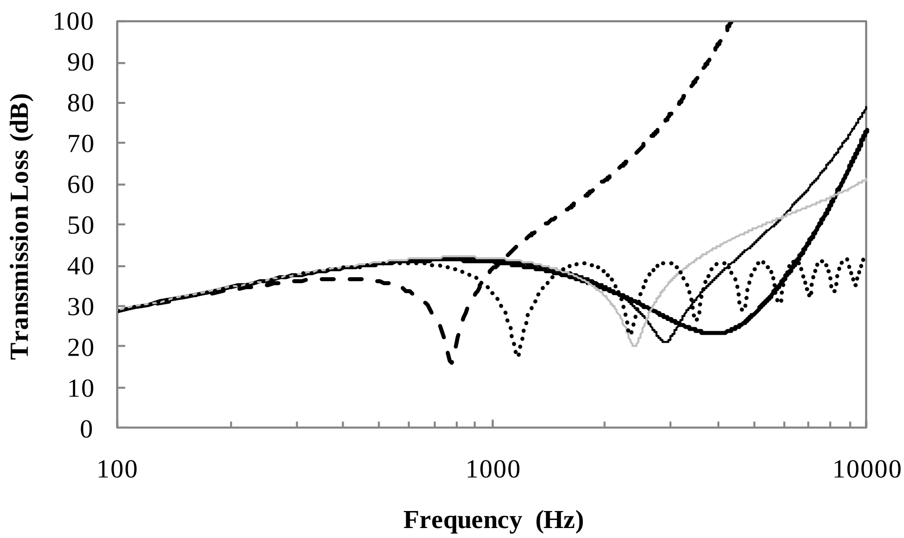

FIG.6. TL properties estimated based on the analytical solution for 78°sound incidence with the panel loss factor η=0.02.

------, Panel A ; ——, Panel B' ; ——, Panel B" ; ——, Panel B ; ··········, Panel C.

C.TRANSMISSION IN DIFFUSE FIELD

TL characteristics in the diffuse field, which are more important for practical problems, should be considered. The TL characteristics of the five kinds of panels shown in Table 1 were calculated in the field incidence condition based on the method shown in Appendix A. The loss factor was assumed to be 0.02, and the increment of incident angles for evaluating the average transmission ratio was 0.1°. The results are shown in Figure 6. Similar to the results of the previous section, in the TL of type B', the most visible TL reduction is shown. In contrast to Sharp's results, many dips exist in the TL for type C, where the shear stiffness is sufficiently low.

For sound transmission in the diffuse field, the influence of shallow incident angle conditions, in which the transmission coefficients are higher, is more dominant, and thus the TL in the field incidence condition has the same tendency as that in the plane wave incident condition at the incident angle of 78°, which is the upper limit angle for evaluating the field incidence condition.

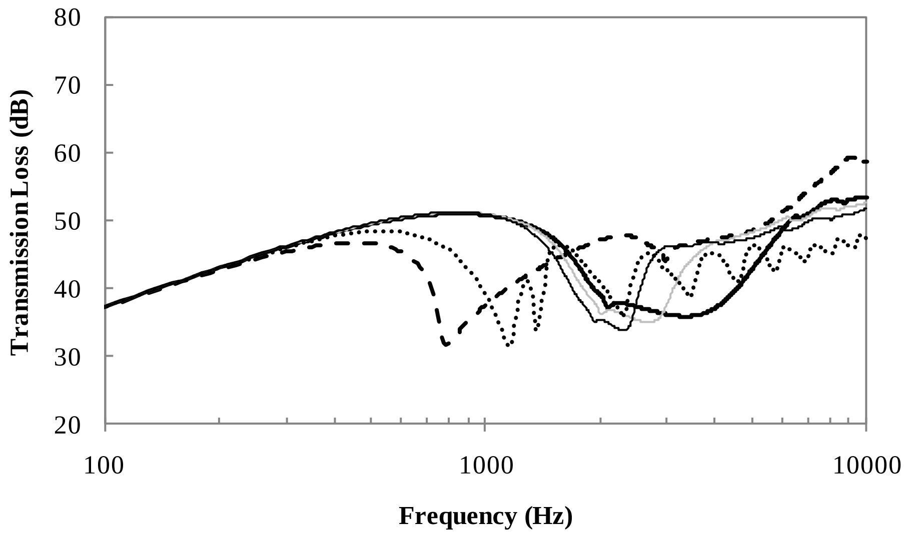

FIG.7. TL properties estimated based on the analytical solution in the field incidence condition with a panel loss factor η of 0.02.

------, Panel A ; ——, Panel B' ; ——, Panel B" ; ——, Panel B ; ··········, Panel C.

C. THE OTHER INVESTIGATIONS

To confirm whether the approximated formula $(0.87+1.12\nu)/(1+\nu)\sqrt{G/\rho}$ can estimate the velocity of flat part in the dispersion curve practically for panels with an arbitrary value of the Poisson ratio, the dispersion properties and TL characteristics were calculated for panels that assumed to have the properties shown in Table 2. The Poisson ratio of panel B-1, B'-1 is 0.2 and that of panel B-2, B'-2 is 0.4. The results are shown in Figure 8. The B'-1, B'-2 panels, where the velocity based on the approximated formula coincides with the incident sound speed in air, have a wider frequency range dip than B-1, B-2. Therefore, it is shown that the value $(0.87+1.12\nu)/(1+\nu)\sqrt{G/\rho}$ is a good approximation to the velocity of the flat part in a dispersion curve and that the TL of the thick panel decreases most drastically in the high frequency range when it coincides with the forcing wave speed.

TABLE II. Properties of panels with poison ratio of 0.2 and 0.4.

Type	G(N/m^2)	v	Wave Speed Condition
B-1	1.476e8	0.2	$\sqrt{\frac{G}{\rho}} = c_0 / \sin(78°)$
B'-1	1.776e8	0.2	$\frac{0.87 + 1.12v}{1+v}\sqrt{\frac{G}{\rho}} = c_0 / \sin(78°)$
B-2	1.476e8	0.4	$\sqrt{\frac{G}{\rho}} = c_0 / \sin(78°)$
B'-2	1.665e8	0.4	$\frac{0.87 + 1.12v}{1+v}\sqrt{\frac{G}{\rho}} = c_0 / \sin(78°)$

Note: ρ=1200kg/m^2 , h=0.15m , c_0=343m/s

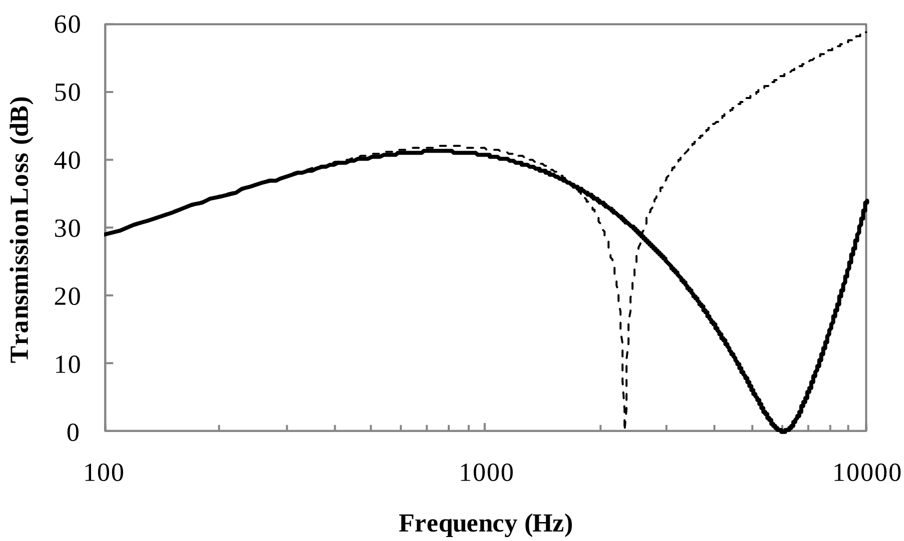

(a) Comparison between B-1 and B'-1: ············, Panel B-1 ; ——, Panel B'-1.

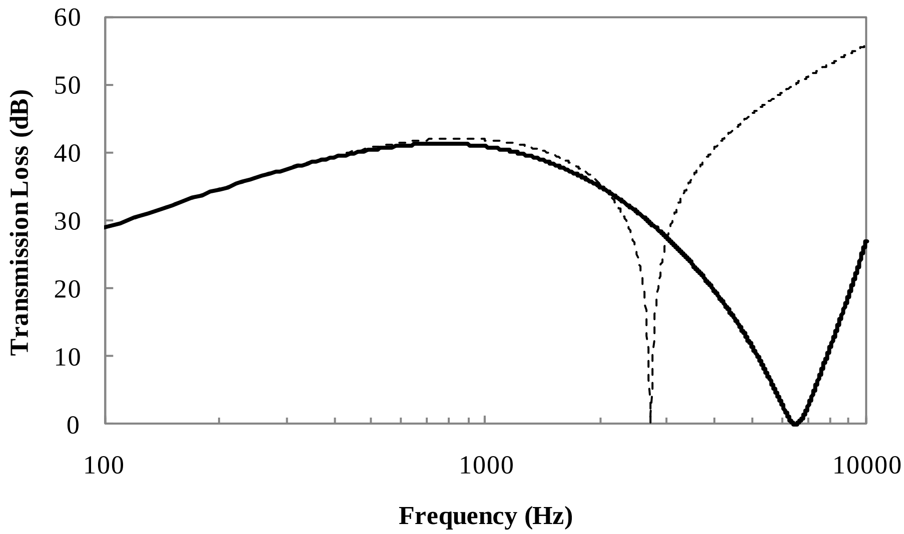

(b) Comparison between B-2 and B’-2: ·········, Panel B-2 ; ——, Panel B’-2.

FIG.8. TL properties comparison for Poisson ratios of 0.2 and 0.4.

For thin panels, it is well-known that no dips in the TL curve appear at the 0° sound incidence condition. However, for thick panels, the TL curve in that condition has many dips, as shown in Figure 9 because of the many branches over the flat part in the dispersion curve. This characteristic does not depend on the panel material property, which is common for the thick panels used in this investigation. Sharp’s model cannot show the TL dips in the 0° incidence condition, as in Figure 10.

To improve the TL for thick panels in the high frequency range, the approach to increase the stiffness of panels is effective, as shown in Figure 7, though the opposite approach is commonly effective for thin panels. Sharp’s model cannot show this characteristic. Although the stiffest panel A has the highest TL in the high frequency range of more than 2 kHz in Figure 7, the softest panel C shows the highest TL in Figure 2, which shows the predictions based on Sharp's model.

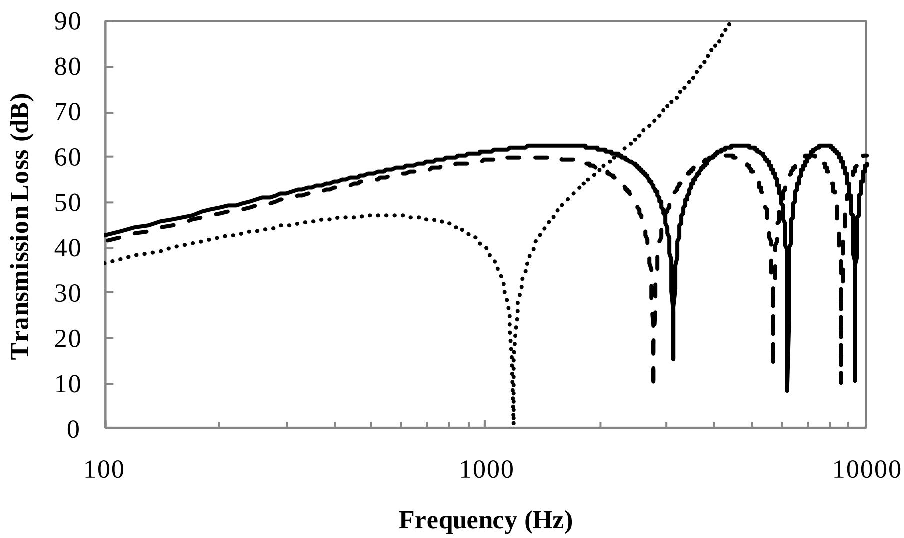

FIG.9. TL properties at 0°, 30° and 60° sound incidence conditions for panel A estimated based on the analytical solution: ——, 0°; ------, 30°; ············, 60°.

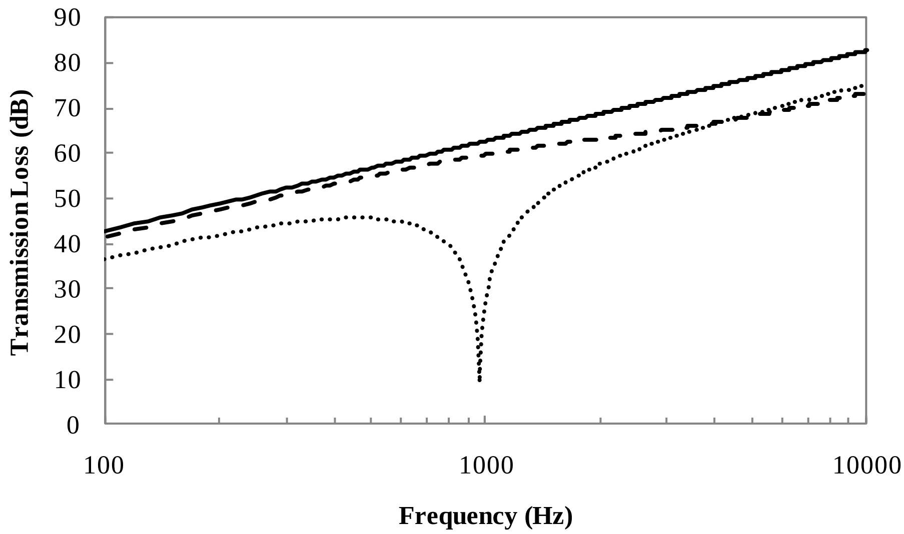

FIG.10. TL properties at 0° , 30° and 60° sound incidence conditions for panel A estimated based on Sharp's impedance model: ——, 0°; ------, 30°; ··········, 60°.

IV. CONCLUSIONS

Investigation of the detailed dispersion characteristics of thick panels leads to a proper understanding for the TL behaviour for them and the following conclusions.

・When the velocity of the flat part in the dispersion curve, which is approximated as $(0.87+1.12\nu)/(1+\nu)\sqrt{G/\rho}$, coincides with the forcing wave speed caused by the incident sound, the TL of the thick panel decreases most drastically in the high frequency range.

・The approach to increasing the stiffness of thick panels is effective for increasing the TL for the panel, and the TL for thick panels at a 0° sound incidence does not have good properties, which are different than the common characteristics of thin panels because of the many branches existing in the high velocity range over the flat part in the dispersion curve of a thick panel.

APPENDIX A : TRANSMISSION LOSS CALCULATION

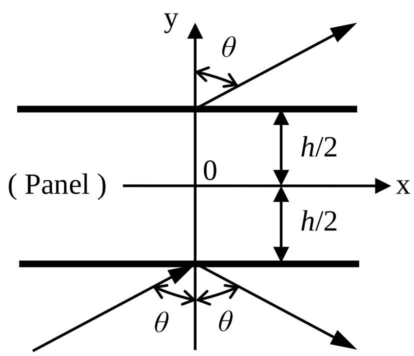

FIG.A-1. Sound transmission through a panel at an incident angle θ.

Fig. A-1 illustrates a plane acoustic wave impinging upon a panel of thickness h at an incidence angle θ. The relation between the pressure P_1, velocity perpendicular to the surface v_1 on the incident side and corresponding variables on the transmitted side, P_2,v_2 is described as follows[13].

$$\begin{bmatrix} P_1 \\ v_1 \end{bmatrix} = \begin{bmatrix} F_{11}(\theta) & F_{12}(\theta) \\ F_{21}(\theta) & F_{22}(\theta) \end{bmatrix} \begin{bmatrix} P_2 \\ v_2 \end{bmatrix} \tag{A-1}$$

Assuming that the characteristic impedance of each side is $Z_0=\rho_0 c_0$, the transmission coefficient at a given angle of incidence θ is shown as follows.

$$\tau_\theta = \left| \frac{2}{F_{11}(\theta) + F_{12}(\theta)/Z_{0\theta} + Z_{0\theta}/F_{21}(\theta) + F_{22}(\theta)} \right| \tag{A-2}$$

where

$$Z_{0\theta} = Z_0/\cos\theta$$

From these expressions, the transmission loss at the incident angle θ is shown as follows.

$$\mathrm{TL}_\theta = \text{-}10\log \tau_\theta \tag{A-3}$$

In the case of a diffuse field excitation with an incidence angle θ varying from 0 to θ_f, the transmission coefficient τ_d is defined by

$$\tau_d = \frac{\int_0^{\theta_f} \tau_\theta \cos\theta \sin\theta d\theta}{\int_0^{\theta_f} \cos\theta \sin\theta d\theta} \tag{A-4}$$

The field incidence transmission loss is obtained by letting θ_f be 78°, so the expression is as follows.

$$\mathrm{TL}_f = \text{-}10\log \left(\frac{\int_0^{78^\circ} \tau_\theta \cos\theta \sin\theta d\theta}{\int_0^{78^\circ} \cos\theta \sin\theta d\theta} \right) \tag{A-5}$$

When the deformation of a whole plate is the main mechanism for transmission, v_1 is almost equal to v_2, and each element of the matrix (A-1) is approximated as follows based on the reciprocity and the symmetric property.

$$F_{11}(\theta) = 1$$
$$F_{12}(\theta) = Z$$
$$F_{21}(\theta) = 0$$
$$F_{22}(\theta) = 1$$

where Z is the panel impedance defined by v_1 ($=v_2$)/(P_1- P_2).

APPENDIX B: ANALYTICAL SOLUTION FOR (A-1) MATRIX

In the case shown in Fig. A-1, the wave in the panel is described by the following displacement potentials [14].

$$\begin{aligned} \Phi &= \mathrm{e}^{\mathrm{j}(\xi x-\omega t)}\{A\sin\, \alpha y + B\cos \alpha y\} \\ H_Z &= \mathrm{j}\,\mathrm{e}^{\mathrm{j}(\xi x-\omega t)}\{C\sin\, \beta y + D\cos \beta y\} \end{aligned} \tag{B-1}$$

where ξ is the wave number in the x direction, ω is the angle frequency, A～D are unfixed constants and α ,β are given as follows.

$$\alpha = \sqrt{\frac{\omega^2}{{c_1}^2} - \xi^2}$$

$$\beta = \sqrt{\frac{\omega^2}{{c_2}^2} - \xi^2}$$

c_1,c_2 are defined as

$$c_1 = \sqrt{\frac{\lambda + 2G}{\rho}}$$

$$c_2 = \sqrt{\frac{G}{\rho}}$$

where λ , G indicate the Lamé constants and ρ indicates the density of the material of the panel. λ is expressed as follows.

$$\lambda = \frac{Ev}{(1+v)(1-2v)}$$

Here, the loss factor η can be introduced using the complex elasticity $E(1+\mathrm{j}\eta)$,$G(1+\mathrm{j}\eta)$.

The displacements in the x and y directions are described based on the potentials as follows.

$$u_x = \frac{\partial \Phi}{\partial x} + \frac{\partial H_Z}{\partial y}$$
$$u_y = \frac{\partial \Phi}{\partial x} - \frac{\partial H_Z}{\partial y} \qquad \text{(B-2)}$$

The stresses are expressed based on these displacements as follows.

$$\tau_{yy} = (\lambda + 2G)\frac{\partial u_y}{\partial y} + \lambda \frac{\partial u_x}{\partial x}$$
$$\tau_{yx} = G\left(\frac{\partial u_y}{\partial x} + \frac{\partial u_x}{\partial y}\right) \qquad \text{(B-3)}$$

From the above expression, the following relations are obtained.

$$\boldsymbol{v}^T = \mathrm{e}^{\mathrm{j}(\xi x - \omega t)} \cdot \boldsymbol{M} \cdot \boldsymbol{W}^T \qquad \text{(B-4)}$$

Where

$$\boldsymbol{v} = \begin{bmatrix} \tau_{yy} & \tau_{yx} & \frac{\partial u_x}{\partial t} & \frac{\partial u_y}{\partial t} \end{bmatrix}$$

$$\boldsymbol{W} = \begin{bmatrix} A & B & C & D \end{bmatrix}$$

$$\boldsymbol{M} = \begin{bmatrix} G\left(\xi^2 - \beta^2\right)\sin\alpha y & G\left(\xi^2 - \beta^2\right)\cos\alpha y & 2G\beta\xi\cos\beta y & -2G\beta\xi\sin\beta y \\ 2\mathrm{j}G\xi\cos\alpha y & -2\mathrm{j}G\alpha\xi\sin\alpha y & \mathrm{j}G\left(\xi^2 - \beta^2\right)\sin\beta y & \mathrm{j}G\left(\xi^2 - \beta^2\right)\cos\beta y \\ \omega\xi\sin\alpha y & \omega\xi\cos\alpha y & \omega\beta\xi\cos\beta y & -\omega\beta\xi\sin\beta y \\ -\mathrm{j}\omega\alpha\cos\alpha y & \mathrm{j}\omega\alpha\sin\alpha y & -\mathrm{j}\omega\xi\sin\beta y & -\mathrm{j}\omega\xi\cos\beta y \end{bmatrix}$$

From (B-4), the following relations are obtained.

$$\boldsymbol{v}^T\left(x,-h/2\right) = \boldsymbol{M}\left(-h/2\right)\cdot\boldsymbol{M}\left(h/2\right)^{-1}\cdot\boldsymbol{v}\left(x,h/2\right)^T \tag{B-5}$$

From (B-5) and the following conditions, the relation (B-6) is given.

$$\begin{aligned} &\tau_{yx}(-h/2) = \tau_{yx}(h/2) = 0 \\ &\tau_{yy}(-h/2) = p_1, \tau_{yy}(h/2) = p_2 \\ &\frac{\partial u_y}{\partial t}(-h/2) = v_1, \frac{\partial u_y}{\partial t}(h/2) = v_2 \end{aligned}$$

$$\begin{bmatrix} p_1 \\ v_1 \end{bmatrix} = \begin{bmatrix} N_{11} - N_{13}\cdot\dfrac{N_{21}}{N_{23}} & N_{14} - N_{13}\cdot\dfrac{N_{24}}{N_{23}} \\ N_{41} - N_{43}\cdot\dfrac{N_{21}}{N_{23}} & N_{44} - N_{43}\cdot\dfrac{N_{24}}{N_{23}} \end{bmatrix} \begin{bmatrix} p_2 \\ v_2 \end{bmatrix} \tag{B-6}$$

where N_{ij} are the elements of the matrix $\boldsymbol{N} = \boldsymbol{M}\left(-h/2\right)\cdot\boldsymbol{M}\left(h/2\right)^{-1}$

By using the relation $\xi = k\sin\theta$, (B-6) correspond to (A-1).

Accordingly, based on (B-6), the TL can be obtained by the process shown in Appendix A.

As shown in Appendix A, the (1,2) element of the matrix corresponds to the panel impedance, and thus, by setting the (1,2) element to 0, the wave propagating velocity can be obtained using the relation $c=\omega\xi$.

The expression for the (1,2) element is as follows.

$$
\begin{aligned}
Z &= N_{14} - N_{13} \cdot \frac{N_{24}}{N_{23}} \\
&= \frac{\mathrm{j} c_2{}^2 G}{\omega^3 \alpha} \cdot \frac{K_0}{4\alpha\beta\xi^2 \sin(\alpha h) + \left(\xi^2 - \beta^2\right)^2 \sin(\beta h)}
\end{aligned}
$$

where

$$K_0 = K_1 \left\{ 4\alpha\beta\xi^2 + \left(\xi^2 - \beta^2\right)^2 \right\} + \left(K_2 - K_1\right) \left\{ 8\alpha\beta\xi^2 \left(\xi^2 - \beta^2\right)^2 \right\}$$

where K_1 and K_2 are as follows.

$$K_1 = \sin(\alpha h) \sin(\beta h)$$

$$K_2 = 1 - \cos(\alpha h) \cos(\beta h)$$

REFERENCES

[1]G.Kurtze and B.G.Watters, “New wall design for high transmission loss or high damping,” J. Acoust. Soc.Am. **31** ,739-748 (1959).

[2]K.H.Heron, “Acoustic radiation from honeycomb sandwich plates,” Fifth European Rotorcraft and Powered Lift Aircraft Forum 65.1-15 (1979).

[3]Evan B.Davis, “Designing honeycomb panels for noise control,”AIAA-99-1917,792-800 (1999).

[4]P.Wennhage,”Structural-acoustic optimization of sandwich panels,” KTH Report 2001-05 (2001).

[5]Jeong-Woo Kim and J.S.Bolton, ”Free wave propagation in sandwich-panels with poro-elastic cores,” Noise-Con 2004 ,651-662 (2004).

[6]Shankar Rajaram, Tongan Wang and Steven Nutt,” Sound transmission loss of honeycomb sandwich panels” Noise Control Eng. J. ,**54** ,106-115 (2006).

[7]B.H.Sharp,” A study of techniques to increase the sound insulation of building elements,” Wyle Laboratories Report WR73-5 (1973).

[8]B.H.Sharp and J.W.Beauchamp,” The transmission loss of multilayer structures,” J. Sound Vib. **9**,383-392 (1969) .

[9]D.L.Folds and C.D.Loggins,” Transmission and reflection of ultrasonic waves in layered media,” J. Acoust. Soc.Am. **62** ,1102-1109 (1977).

[10]B.Brouard, D.Lafarge and J.-F.Allard,” A General method of modeling sound propagation in layered media,” J. Sound Vib.**183**,129-142 (1995) .

[11]F.G.Leppington,K.H.Heron etc.,” Resonant and non-resonant acoustic properties of elastic panels.2 The transmission problem,” Proceeding of R.Soc.Lond.A412 ,309-337 (1987).

[12]E.C.Sewell,” Transmission of reverberant sound through a single –leaf partition surrounded by an infinite rigid baffle,” J. Sound Vib.**12**,21-32 (1970) .

[13]Yukio Hamada and Hideki Tachibana,” Analysis of sound transmission loss of multiple structures by four-terminal network theory,” Inter-Noise85 ,693-695 (1985).

[14]K.F.Graff Wave Motion in Elastic Solids ,(Dover, New York ,1991)